

Structural Preferences of Single-Walled Silica Nanostructures: Nanospheres and Chemically Stable Nanotubes

Mikko Linnolahti,* Niko M. Kinnunen, and Tapani A. Pakkanen^[a]

Abstract: Structural preferences of single-walled and coordinatively saturated spherical and tubular nanostructures of silica have been determined by ab initio calculations. Two families of spherical $(\text{SiO}_2)_n$ clusters derived from Platonic solids and Archimedean polyhedra are depicted, with n ranging from 4–120. The analogue of a truncated icosidodecahedron, I_h -symmetric

$\text{Si}_{120}\text{O}_{240}$, is favored in energy, closely followed by the I_h -symmetric $\text{Si}_{60}\text{O}_{120}$ -truncated icosahedron. The silica nanotubes derived from spherical clusters are capped by Si_2O_2 rings, whereas the

tubular section consists of single oxygen bridges. Periodic studies performed with open-ended silica nanotubes and the α -quartz polymorph of silica, along with a comparisons to fullerenes and carbon nanotubes, suggest that tubes with diameters of approximately 1 nm should be chemically stable.

Keywords: ab initio calculations • nanostructures • silica • structure elucidation

Introduction

Inorganic nanotubes constitute a diverse class of materials; tubes of various chalcogenides, oxides, nitrides, halides, and metals have been synthesized previously.^[1] Silica, being a highly abundant and versatile material, is no exception. In addition to its complex polymorphism it is capable of forming various nanostructures, including silica gel,^[2] mesoporous materials,^[3] individual nanotubes,^[4] nanowires, and nanospheres.^[5] Efforts have been made to synthesize silica nanotubes with different morphologies,^[6] and to study their growth mechanism.^[7] The tubes are multiwalled with diameters of up to hundreds of nanometers, and the use of a template is often required to achieve shape control.^[8,9] So far, single-walled silica nanotubes have not been obtained.

Because of the versatility of silica, structure elucidation of silica nanostructures is a challenge. To take control of its structural characteristics, it is useful to begin with small clusters. Several theoretical papers on structural preferences of $(\text{SiO}_2)_n$ clusters have been reported during the last decade. It is now known that linear D_{2h} - and D_{2d} -symmetric chains, composed of Si_2O_2 rings with double oxygen bridges and Si=O terminal ends, are favored when $n < 7$.^[10] This is due to

the large number of coordinatively saturated silicon and oxygen atoms in short chains among the isomers. Because of an exponential increase in the number of possible isomers as a function of n , comprehensive analysis of all of the isomers of larger oligomers is hardly feasible. Nevertheless, several structural families have been proposed: 1) fully coordinated Si_2O_2 -based rings, which possess greater stability than the corresponding chains starting from $n > 11$,^[11] 2) chains and rings containing Si_3O_3 rings,^[12] 3) oxygen-terminated cages,^[13] and 4) coordinatively saturated cages up to $n = 24$.^[14,15] While not always lower in energy, the coordinatively saturated structures appear the most reasonable candidates, due to the absence of reactive Si=O end groups.

In the theoretical approach described here, our focus is on the determination of molecular structures of single-walled coordinatively saturated silica nanostructures. Nanospheres were first derived from regular polyhedra, then the spheres were elongated to nanotubes. The relative stability of the nanostructures and infinitely long tubes were then estimated on the basis of a periodic calculation of crystalline silica.

Computational Methods

A preliminary optimization of nanospheres was performed by the HF/3-21G^(*) method, followed by verification of the character of stationary points by frequency calculations. The true minima were reoptimized by Hartree-Fock (HF) and hybrid density functional B3LYP methods, in

[a] Dr. M. Linnolahti, N. M. Kinnunen, Prof. T. A. Pakkanen
Department of Chemistry, University of Joensuu
P.O. Box 111, 80101 Joensuu (Finland)
Fax: (+358) 13-251-3390
E-mail: Mikko.Linnolahti@joensuu.fi

combination with modified 6-21G* and 6-31G* basis sets for Si and O, respectively. The basis sets applied have been specifically optimized for silica by Civalleri et al.,^[16] optimized basis sets being necessary for periodic calculations. All calculations, including the periodic ones, were performed by Gaussian 03 software.^[17]

Results and Discussion

Derivation of $(\text{SiO}_2)_n$ nanospheres from regular polyhedra:

Single-walled silica nanospheres were derived from Platonic solids and Archimedean polyhedra. Platonic solids are usually denoted by the notation $\{p, q\}$, in which p is the number of sides in each face and q is the number of faces that meet at each vertex. We have previously demonstrated, by using Al_2O_3 nanostructures as an example, that nanospheres with 2:3 stoichiometry can be derived from Platonic solids when $q=3$.^[18] Without losing the original symmetry of the polyhedron, this was done by placing metal atoms into the vertices of the polyhedron, followed by connection of the vertices by means of oxygen bridges. In the case of silica with a stoichiometry of 1:2, the methodology is only applicable for Platonic solids when $q=4$ (for octahedra). As an alternative building strategy, the required 1:2 stoichiometry can be produced from Platonic solids when $q=3$, by introducing double oxygen bridges between every second pair of Si vertices (Figure 1). The latter methodology does not, however, preserve the original symmetry of the parent Platonic solid.

In a similar way, $(\text{SiO}_2)_n$ nanospheres can be derived from Archimedean polyhedra. In the case of polyhedra in which

three faces meet at each vertex, nanostructures with alternating single and double oxygen bridges are formed, whereas the polyhedra with four faces meeting at each vertex produce structures with single oxygen bridges. It is worth noting that, unlike for Platonic solids, the original symmetry is always preserved. The methodology for deriving silica nanospheres from Archimedean polyhedra is illustrated in Figure 2. In addition to the aforementioned alumina,^[18] we have recently applied a similar approach to magnesium dichloride^[19] and aluminoxane^[20] cages.

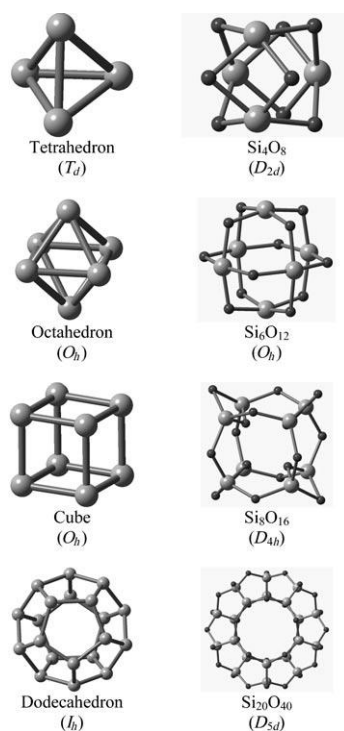


Figure 1. From Platonic solids to silica nanostructures.

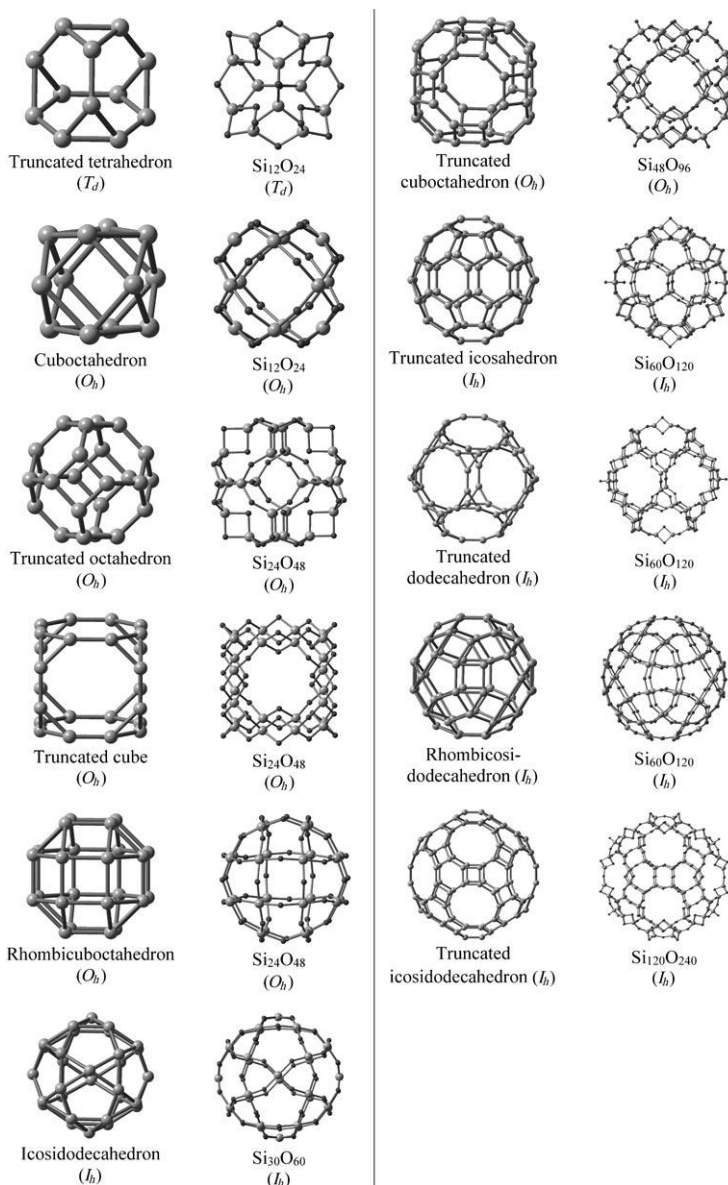


Figure 2. From Archimedean polyhedra to silica nanostructures.

Relative stabilities of $(\text{SiO}_2)_n$ nanospheres: The relevance of the derived silica nanospheres was first examined by using the HF/3-21G* theory. Frequency calculations indicated that the tetrahedron, cube, cuboctahedron, rhombicuboctahe-

dron, icosidodecahedron, and rhombicosidodecahedron counterparts of silica, each possessing one or more imaginary frequencies, are not true minima. The remaining nine clusters, with no imaginary frequencies, were optimized further by both the HF and B3LYP methods, in combination with the basis set developed by Civalleri et al.^[16] Table 1

Table 1. Structures, diameters, and stabilities relative to α -quartz for optimized silica nanostructures derived from regular polyhedra.

Parent polyhedra	Symmetry	Formula	n	Rings	Diameter [nm] ^[a]	$\Delta E_{\text{HF}}/n$ ^[b] [kJ mol ⁻¹]	$\Delta E_{\text{B3LYP}}/n$ ^[b] [kJ mol ⁻¹]
octahedron	O_h	Si ₆ O ₁₂	6	8 × Si ₃ O ₃	0.47	568.3	483.9
truncated tetrahedron	T_d	Si ₁₂ O ₂₄	12	6 × Si ₂ O ₂ , 4 × Si ₃ O ₃ , 4 × Si ₆ O ₆	0.81	202.3	177.7
dodecahedron	D_{5d}	Si ₂₀ O ₃₀	20	10 × Si ₂ O ₂ , 12 × Si ₅ O ₅	0.97	126.9	109.9
truncated octahedron	O_h	Si ₂₄ O ₄₈	24	12 × Si ₂ O ₂ , 6 × Si ₄ O ₄ , 8 × Si ₆ O ₆	1.07	112.5	97.1
truncated cube	O_h	Si ₂₄ O ₄₈	24	12 × Si ₂ O ₂ , 8 × Si ₃ O ₃ , 6 × Si ₈ O ₈	1.14	120.5	105.0
truncated cuboctahedron	O_h	Si ₄₈ O ₉₆	48	24 × Si ₂ O ₂ , 12 × Si ₄ O ₄ , 8 × Si ₆ O ₆ , 6 × Si ₈ O ₈	1.50	103.7	90.8
truncated icosahedron	I_h	Si ₆₀ O ₁₂₀	60	30 × Si ₂ O ₂ , 12 × Si ₅ O ₅ , 20 × Si ₆ O ₆	1.62	89.5	78.9
truncated dodecahedron	I_h	Si ₆₀ O ₁₂₀	60	30 × Si ₂ O ₂ , 20 × Si ₃ O ₃ , 12 × Si ₁₀ O ₁₀	1.80	101.0	88.6
truncated icosidodecahedron	I_h	Si ₁₂₀ O ₂₄₀	120	60 × Si ₂ O ₂ , 30 × Si ₄ O ₄ , 20 × Si ₆ O ₆ , 12 × Si ₁₀ O ₁₀	2.34	89.0	78.7

[a] Measured from B3LYP optimized structures. [b] Modified 6-21G* (Si) and 6-31G* (O) basis sets, optimized by Civalleri et al. (Ref [16]).

summarizes the structures, and relative stabilities of relevant silica nanospheres derived from regular polyhedra. The energies per SiO₂ unit are given relative to α -quartz, which is the lowest energy polymorph of silica, as demonstrated by periodic calculations of Catti and co-workers.^[21] Several other theoretical studies are available for the silica polymorphs as well.^[22]

From the polyhedra, in which four faces meet at each vertex, the O_h -symmetric analogue of octahedron (SiO₂)₆ is the only true minimum. The structure consists of eight Si₃O₃ rings, and has a diameter of 0.47 Å. All other structures belong to the family of polyhedra with three faces meeting at each vertex, for which the required stoichiometry of Si/O = 1:2 is satisfied by alternating single and double oxygen bridges, therefore producing $n/2$ Si₂O₂ rings. The latter structural family is clearly favored over the octahedron, which is strongly destabilized by the unavoidable square-planar orientation of the four-coordinated Si atoms. However, nanostructures with alternating single and double oxygen bridges do accommodate the preferable tetrahedral orientation, thus

lowering their stability to below 100 kJ mol⁻¹ per SiO₂ unit from that of α -quartz, independent of the method applied. Compared to the B3LYP method, the HF method yields lower stability for the clusters, while maintaining exactly the same order of stability.

Followed by the unstable octahedron, the analogue of the truncated tetrahedron possesses the next highest relative energy. The structure is destabilized because of the repulsion of the double oxygen bridges pointing inwards in the small cage. The stability generally improves as a function of the cluster size, the I_h -symmetric Si₁₂₀O₂₄₀ analogue of a truncated icosidodecahedron being favored, closely followed by the I_h -symmetric Si₆₀O₁₂₀ counterpart of a truncated icosahedron. Both clusters are nanoscale with diameters of 2.34 and 1.62 nm, respectively, and have approximately 80 kJ mol⁻¹ more energy per SiO₂ unit than α -quartz. The Si–O bond lengths in the Si₁₂₀O₂₄₀ truncated icosidodecahedron range from 1.63 Å in single oxygen bridges, to 1.67 Å in double oxygen bridges, which are close to the bond lengths of 1.61 Å in α -quartz.^[23] Excluding the Si₂O₂ rings, the O–Si–O angles can accommodate optimal tetrahedral orientation, the values range from 108.7 to 114.7°. The Si–O–Si angles,

again with the exception of Si₂O₂ rings, adopt values of 139.0 or 147.6°, similar to the angle of 143.7° for α -quartz. Apparently, the major source of destabilization, compared to the crystalline form, is due to $n/2$ Si₂O₂ rings, that is, the double oxygen bridges, found at the silica surfaces under severe conditions.^[24] Theoretical studies on the silica counterparts of the Si₁₂O₂₄-truncated tetrahedron, Si₂₄O₄₈-truncated octahedron, and Si₂₄O₄₈-truncated cube have been reported previously by Bromley,^[14] who concluded that coordinatively saturated cages become favored over the Si=O terminated clusters when $n=24$.

From (SiO₂)_n nanospheres to nanotubes: Single-walled silica nanotubes were first derived by elongation of the parent Platonic solids to obtain a molecular formula of Si₇₀O₁₄₀, thus producing two distinct families of nanotubes (Figure 3). The D_{4h} -symmetric tube formed from the octahedron contains only single oxygen bridges, and is closed with a nearly square-planar SiO₄ unit, the tubular section consisting of Si₄O₈ repetitive units in the form of Si₄O₄ rings. Similar to

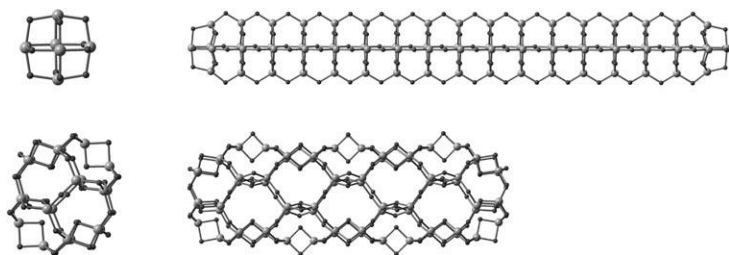


Figure 3. Derivation of two families of closed silica nanotubes by elongation of polyhedral clusters.

its dodecahedral counterpart, the D_{5h} -symmetric tube contains $n/2$ Si_2O_2 rings. The tube is closed with halves of the dodecahedron. The tubular section, with a repetitive unit of $\text{Si}_{10}\text{O}_{20}$, is formed from rings of six Si atoms.

Relative stabilities at the HF level, with respect to α -quartz, are given in Figure 4, for the two families of silica nanotubes as a function of the number of SiO_2 units up to

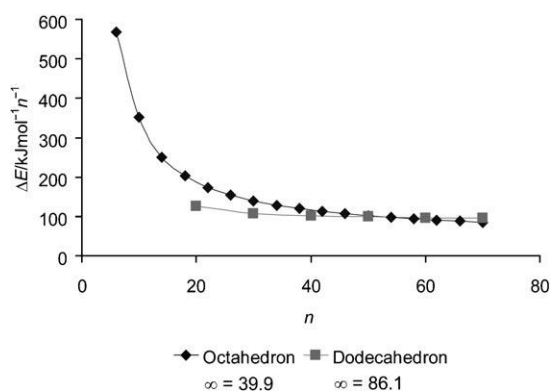


Figure 4. Stabilities relative to α -quartz as a function of tube length for closed $(\text{SiO}_2)_n$ nanotubes, derived from an octahedron and a dodecahedron.

$n = 70$. As far as the polyhedral silica clusters are concerned, the dodecahedron is clearly favored over the octahedron. This order is reversed for silica nanotubes with approximately 60 SiO_2 units or more. Faster stabilization of octahedra suggests that single oxygen bridges are preferred over doubly bridging ones. Apparently, the silica counterpart of the octahedron suffers from square-planar SiO_4 capping, and the faster gain in stability, as a function of tube length, is due to the increased relative proportion of the preferable tubular section. The effect of capping can be removed by extrapolation of the tube to an infinite length. In the case of the octahedron, the infinitely long tube lies $39.9 \text{ kJ mol}^{-1} n^{-1}$ above α -quartz, whereas the infinitely long tube derived from dodecahedron is much less stable, lying $86.6 \text{ kJ mol}^{-1} n^{-1}$ above the crystalline form.

Since both families of tubes presented have their pros and cons, it is convenient to combine their favorable structural components, that is, the tubular section of single oxygen bridges with the doubly bridging cap. Four such tubes were

considered in this study, and the upper limit was set to 70 SiO_2 units (Figure 5). The relative stabilities of capped silica nanotubes are summarized in Table 2. The doubly

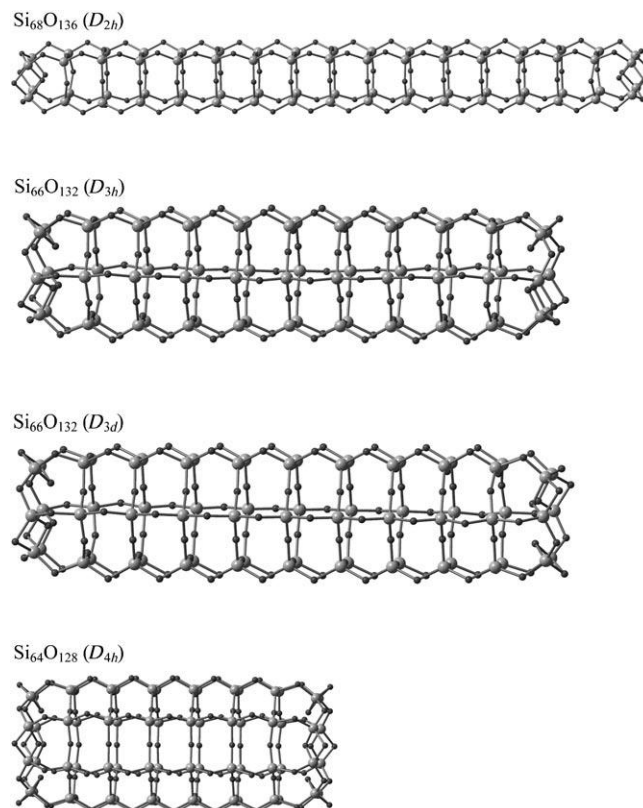


Figure 5. Closed silica nanotubes derived by combining the singly oxygen-bridged tubular section with doubly bridging caps.

Table 2. Stabilities relative to α -quartz for the longest capped silica nanotubes studied.

Type	Symmetry	Formula	n	$\Delta E_{\text{HF}}/n$ [kJ mol^{-1}]
elongated octahedron	D_{4h}	$\text{Si}_{70}\text{O}_{140}$	70	85.4
elongated dodecahedron	D_{5h}	$\text{Si}_{70}\text{O}_{140}$	70	95.1
combined single/double-bridging	D_{2h}	$\text{Si}_{68}\text{O}_{136}$	68	76.7
combined single/double-bridging	D_{3h}	$\text{Si}_{66}\text{O}_{132}$	66	69.4
combined single/double-bridging	D_{3d}	$\text{Si}_{66}\text{O}_{132}$	66	69.4
combined single/double-bridging	D_{4h}	$\text{Si}_{64}\text{O}_{128}$	64	76.0

oxygen-bridging caps halve the axis of rotation. The opposing oxygen double bridges can be aligned or antialigned, resulting in D_{3h} or D_{3d} symmetry, respectively, for tubes containing Si_6O_6 rings in the tubular section. These tubes are similar to the elongated $\text{Si}_{12}\text{O}_{24}$, $\text{Si}_{18}\text{O}_{36}$, and $\text{Si}_{24}\text{O}_{48}$ cages reported by Bromley,^[14] who found the lowest energy isomers to have their bridges antialigned (D_{3d}). While this is true for very short tubes, which originate due to repulsions between opposite bridges, it becomes negligible at longer separation. In the case of the $\text{Si}_{66}\text{O}_{132}$ tube, the isomers are separated by an energy difference of only $0.003 \text{ kJ mol}^{-1}$ in favor of D_{3h} .

De Leeuw et al. have employed the D_{3h} -type $\text{Si}_{36}\text{O}_{72}$ tube to study the effect of hydration on the stability of the tube.^[26] The authors justified their model selection on the basis of similarities with α -quartz and microporous silicate materials. Their conclusion, that the side of the tube is resistant to attack by water while the ends are not, is clearly supported by our calculations. Furthermore, this indicates that the silica nanospheres presented above, with alternating single and double oxygen bridges, might be kinetically unstable. Tubes containing Si_4O_4 or Si_8O_8 rings in the tubular section were studied only in D_{2h} and D_{4h} symmetry, respectively, because of the marginal influence of bridge orientations on the relative stability (Figure 6). The relative stabilities improve in the order $D_{2h} < D_{4h} < D_{3h} = D_{3d}$, suggesting the preference of tubes with a diameter of approximately 0.8 nm.

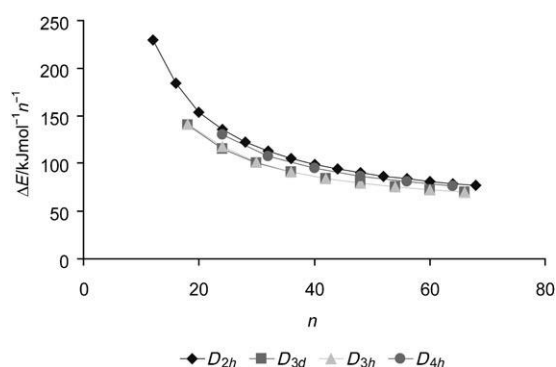


Figure 6. Stabilities relative to α -quartz as a function of tube length for closed $(\text{SiO}_2)_n$ nanotubes derived by combining the singly oxygen-bridged tubular section with doubly bridged caps.

To verify the preferable stability of thin tubes, we performed periodic calculations at both HF and B3LYP levels, optimizing the corresponding open-ended tubes. The relative stability of the tubes was studied as a function of the tube diameter, that is, the repetitive $(\text{SiO}_2)_n$ ring, in which $n=3$ –24 (Table 3 and Figure 7). The sharp decrease in relative energy, when moving from $n=3$ to $n=4$, is followed by small improvements in the stability; this trend continues up

Table 3. Diameters and stabilities relative to α -quartz for infinitely long open-ended silica nanotubes.

Repetitive ring	Symmetry	Diameter ^[a] [nm]	$\Delta E_{\text{HF}}/n$ [kJ mol ⁻¹]	$\Delta E_{\text{B3LYP}}/n$ [kJ mol ⁻¹]
$(\text{SiO}_2)_3$	C_{3v}	0.45	54.8	46.6
$(\text{SiO}_2)_4$	C_{4v}	0.63	45.1	38.7
$(\text{SiO}_2)_5$	C_{5v}	0.69	44.0	38.2
$(\text{SiO}_2)_6$	C_{6v}	0.82	43.8	37.7
$(\text{SiO}_2)_7$	C_{7v}	0.87	43.9	37.6
$(\text{SiO}_2)_8$	C_{8v}	1.00	44.4	37.7
$(\text{SiO}_2)_9$	C_{9v}	1.07	45.3	38.2
$(\text{SiO}_2)_{10}$	C_{10v}	1.18	46.3	38.9
$(\text{SiO}_2)_{12}$	C_{12v}	1.35	48.8	40.8
$(\text{SiO}_2)_{18}$	C_{18v}	1.87	56.0	46.7
$(\text{SiO}_2)_{24}$	C_{24v}	2.43	61.6	51.5

[a] Measured from B3LYP optimized structures.

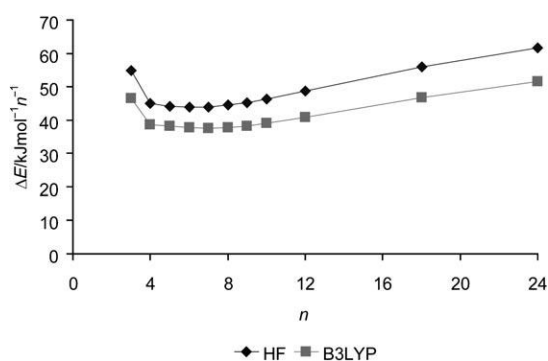


Figure 7. Stabilities relative to α -quartz as a function of the repetitive $(\text{SiO}_2)_n$ ring for open-ended silica nanotubes.

to $n=7$, after which the energy steadily begins to rise. Silica nanotubes, in which $n=3$, 7, and 24, are illustrated in Figure 8. According to B3LYP calculations, the preferred tubes have diameters of around 1 nm, and have energies $< 40 \text{ kJ mol}^{-1} n^{-1}$ above that of α -quartz. The HF method produces practically the same trends, while somewhat lower stabilities are observed, compared to the B3LYP method.

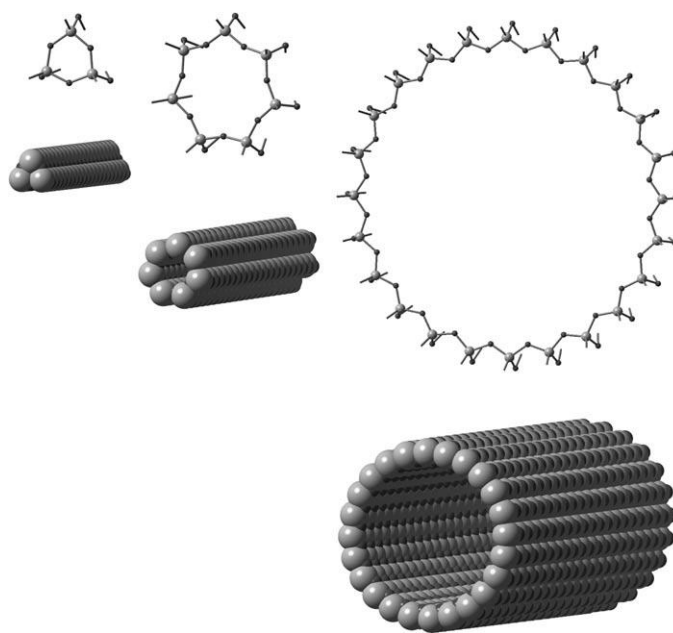


Figure 8. The repetitive $(\text{SiO}_2)_n$ rings and space-filling models of open-ended silica nanotubes, in which $n=3$, 7, and 24.

The practical outcome of a calculated energy difference of $< 40 \text{ kJ mol}^{-1} n^{-1}$ is not easy to estimate, since either thermodynamic or kinetic stability is required for chemical stability. It is apparent that the energies of the tubes are above that of α -quartz, as are the other known polymorphs of silica. From an energetic point of view, how much above is acceptable for the tubes to be within the reach of synthesis is another issue. As a reference, we selected carbon fullerenes and nanotubes, and considered the energy required to

fold a graphene sheet into C_{32} and C_{60} fullerenes, and into an open-ended (5,5) carbon nanotube of infinite length. Full optimizations were performed for each species by using the HF and B3LYP theories.^[27] The C_{32} fullerene, for which experimental evidence is available from anion photoelectron spectroscopy,^[28] has several isomers, the D_3 -symmetric isomer being favored in energy.^[29] The strain energy for the D_3 -symmetric C_{32} is 96.4 kJ mol^{-1} per C atom at the HF level, and 84.4 kJ mol^{-1} per C atom at the B3LYP level. The highly abundant C_{60} fullerene is much more stable, 47.2 kJ mol^{-1} per C atom (HF) and 43.0 kJ mol^{-1} per C atom (B3LYP) above the value of graphene. A significant contributor to the difference between C_{60} and C_{32} is caused by the presence of isolated pentagons in C_{60} . The (5,5) carbon nanotube has a diameter of C_{60} , and so halves of C_{60} are suitable for capping these tubes. In the absence of caps, that is, when an infinitely long open-ended tube is considered, the tube energy lies 22.9 kJ mol^{-1} per C atom and 19.3 kJ mol^{-1} per C atom above the graphene sheet using the HF and B3LYP methods, respectively, to calculate these values. On the basis of this comparison, single-walled silica nanotubes are seen to show high stability.

In the case of fullerenes, kinetic stability plays an important role, as is seen by the high abundance of C_{60} instead of giant fullerenes.^[30] The evaluation of kinetic stability is by no means straightforward, when one considers the numerous reactions the molecules may undergo. The stability of fullerenes has been inspected in terms of HOMO–LUMO energy gaps,^[31] which serve as an indication of the kinetic stability.^[32] Considering the nanostructures of silica, the energy gaps of open-ended silica nanotubes are similar, $8.2\text{--}8.5 \text{ eV}$ at the B3LYP level, being very close to the calculated gap energy of α -quartz, which is 8.6 eV . Agreement with the experimental band gap of approximately 9 eV ^[33] is excellent. Taking this into consideration, the open-ended tubes could be kinetically stable also.

Conclusion

Molecular structures of single-walled silica nanospheres and nanotubes were studied by ab initio HF and hybrid density functional B3LYP methods. Nanospheres were derived from Platonic solids and Archimedean polyhedra, which were elongated to form both capped and open-ended nanotubes. The relative stability of the nanostructures was estimated on the basis of a periodic study on α -quartz, which is the lowest energy polymorph of silica.

Two families of silica nanospheres can be derived: 1) clusters with single bridging and 2) clusters with alternating single and double oxygen bridges. The latter family is clearly favored in energy, due to its ability to adapt SiO_4 fragments with tetrahedral orientation. The lowest relative energy is obtained for the $\text{Si}_{120}\text{O}_{240}$ counterpart of a truncated icosidodecahedron, with an energy of 78.7 kJ mol^{-1} per SiO_2 unit higher than that of α -quartz at the B3LYP level. A major source of destabilization may come from reactive Si_2O_2

rings, which might complicate the synthesis of silica nanospheres.

In contrast to nanospheres, silica nanotubes prefer single oxygen bridges in the tubular section, so the SiO_4 fragments can accommodate a tetrahedral orientation. The tubes are capped by Si_2O_2 rings, considerably decreasing the proportion of reactive sites, especially in the case of long tubes. The effect of the tube caps was removed by periodic calculations on open-ended silica nanotubes, for which the stability was studied as a function of the tube diameter. The highest stability, $< 40 \text{ kJ mol}^{-1}$ per SiO_2 unit above α -quartz at the B3LYP level, was observed for thin tubes with diameters of approximately 1 nm. Comparison to fullerenes and to a (5,5) carbon nanotube suggest that silica nanotubes could be chemically stable.

- [1] C. N. R. Rao, M. Nath, *Dalton Trans.* **2003**, 1–24.
- [2] H. Nakamura, Y. Matsui, *J. Am. Chem. Soc.* **1995**, *117*, 2651–2652.
- [3] H.-P. Lin, C.-Y. Mou, S.-B. Liu, *Adv. Mater.* **2000**, *12*, 103–106.
- [4] M. Harada, M. Adachi, *Z. Mater.* **2000**, *12*, 839–841.
- [5] J. L. Gole, Z. L. Wang, Z. R. Dai, K. Stout, M. White, *Colloid Polym. Sci.* **2003**, *281*, 673–685.
- [6] F. Miyaji, Y. Watanabe, Y. Suyama, *Mater. Res. Bull.* **2003**, *38*, 1669–1680.
- [7] Z. Wang, R. P. Gao, J. L. Gole, J. D. Stout, *Adv. Mater.* **2000**, *12*, 1938–1940.
- [8] F. Miyaji, S. A. Davis, J. P. H. Charmant, S. Mann, *Chem. Mater.* **1999**, *11*, 3021–3024.
- [9] K. J. C. van Bommel, A. Friggeri, S. Shinkai, *Angew. Chem.* **2003**, *115*, 1010–1030; *Angew. Chem. Int. Ed.* **2003**, *42*, 980–999.
- [10] a) J. A. W. Harkless, D. K. Stillinger, F. H. Stillinger, *J. Phys. Chem.* **1996**, *100*, 1098–1103; b) L.-S. Wang, J. B. Nicholas, M. Dupuis, H. Wu, S. D. Colson, *Phys. Rev. Lett.* **1997**, *78*, 4450–4453; c) S. K. Nayak, B. K. Rao, S. N. Khanna, P. Jena, *J. Chem. Phys.* **1998**, *109*, 1245–1250; d) C. Xu, W. Wang, W. Zhang, J. Zhuang, L. Liu, Q. Kong, L. Zhao, Y. Long, K. Fan, S. Qian, Y. Li, *J. Phys. Chem. A* **2000**, *104*, 9518–9524; e) T. S. Chu, R. Q. Zhang, H. F. Cheung, *J. Phys. Chem. B* **2001**, *105*, 1705–1709; f) R. Q. Zhang, T. S. Chu, S. T. Lee, *J. Chem. Phys.* **2001**, *114*, 5531–5536; g) W. C. Lu, C. Z. Wang, V. Nguyen, M. W. Schmidt, M. S. Gordon, K. M. Ho, *J. Phys. Chem. A* **2003**, *107*, 6936–6943.
- [11] S. T. Bromley, M. A. Zwijnenburg, T. Maschmeyer, *Phys. Rev. Lett.* **2003**, *90*, 035502.
- [12] a) W. C. Lu, C. Z. Wang, K. M. Ho, *Chem. Phys. Lett.* **2003**, *378*, 225–231; b) M. W. Zhao, R. Q. Zhang, S. T. Lee, *Phys. Rev. B* **2004**, *69*, 153403–153407.
- [13] a) E. Flikkema, S. T. Bromley, *Chem. Phys. Lett.* **2003**, *378*, 622–629; b) E. Flikkema, S. T. Bromley, *J. Phys. Chem. B* **2004**, *108*, 9638–9645.
- [14] S. T. Bromley, *Nano Lett.* **2004**, *4*, 1427–1432.
- [15] R. A. LaViolette, M. T. Benson, *J. Chem. Phys.* **2000**, *112*, 9269–9275.
- [16] B. Civalieri, C. M. Zicovich-Wilson, P. Ugliengo, V. R. Saunders, R. Dovesi, *Chem. Phys. Lett.* **1998**, *292*, 394–402.
- [17] Gaussian 03, Revision C.02, M. J. Frisch, G. W. Trucks, H. B. Schlegel, G. E. Scuseria, M. A. Robb, J. R. Cheeseman, J. A. Montgomery, Jr., T. Vreven, K. N. Kudin, J. C. Burant, J. M. Millam, S. S. Iyengar, J. Tomasi, V. Barone, B. Mennucci, M. Cossi, G. Scalmani, N. Rega, G. A. Petersson, H. Nakatsuji, M. Hada, M. Ehara, K. Toyota, R. Fukuda, J. Hasegawa, M. Ishida, T. Nakajima, Y. Honda, O. Kitao, H. Nakai, M. Klene, X. Li, J. E. Knox, H. P. Hratchian, J. B. Cross, V. Bakken, C. Adamo, J. Jaramillo, R. Gomperts, R. E. Stratmann, O. Yazyev, A. J. Austin, R. Cammi, C. Pomelli, J. W. Ochterski, P. Y. Ayala, K. Morokuma, G. A. Voth, P. Salvador, J. J. Dannenberg, V. G. Zakrzewski, S. Dapprich, A. D. Daniels, M. C.

- Strain, O. Farkas, D. K. Malick, A. D. Rabuck, K. Raghavachari, J. B. Foresman, J. V. Ortiz, Q. Cui, A. G. Baboul, S. Clifford, J. Cio-slawski, B. B. Stefanov, G. Liu, A. Liashenko, P. Piskorz, I. Komaromi, R. L. Martin, D. J. Fox, T. Keith, M. A. Al-Laham, C. Y. Peng, A. Nanayakkara, M. Challacombe, P. M. W. Gill, B. Johnson, W. Chen, M. W. Wong, C. Gonzalez, J. A. Pople, Gaussian, Inc., Wallingford CT, **2004**.
- [18] M. Linnolahti, T. A. Pakkanen, *Inorg. Chem.* **2004**, *43*, 1184–1189.
- [19] T. N. P. Luhtanen, M. Linnolahti, T. A. Pakkanen, *Inorg. Chem.* **2004**, *43*, 4482–4486.
- [20] M. Linnolahti, T. N. P. Luhtanen, T. A. Pakkanen, *Chem. Eur. J.* **2004**, *10*, 5977–5987.
- [21] M. Catti, B. Civalleri, P. Ugliero, *J. Phys. Chem. B* **2000**, *104*, 7259–7265.
- [22] a) S. Tsuneyuki, M. Tsukada, H. Aoki, Y. Matsui, *Phys. Rev. Lett.* **1988**, *61*, 869–874; b) S. Tsuneyuki, H. Aoki, M. Tsukada, Y. Matsui, *Phys. Rev. Lett.* **1990**, *64*, 776–779; c) R. Nada, C. R. A. Catlow, R. Dovesi, C. Pisani, *Phys. Chem. Miner.* **1990**, *17*, 353–362; d) N. T. Keskar, N. Troullier, J. L. Martins, J. R. Chelikowsky, *Phys. Rev. B* **1991**, *44*, 4081–4088; e) J. C. White, A. C. Hess, *J. Phys. Chem.* **1993**, *97*, 6398–6404; f) F. Liu, S. H. Garofalini, D. King-Smith, D. Vanderbilt, *Phys. Rev. B* **1994**, *49*, 528–534; g) D. R. Hamann, *Phys. Rev. B* **1997**, *55*, 784–793; h) D. Ceresoli, M. Bernasconi, S. Iarlori, M. Parrinello, E. Tosatti, *Phys. Rev. Lett.* **2000**, *84*, 3887–3890; i) G. Pacchioni, *Solid State Sci.* **2000**, *2*, 161–179.
- [23] Y. Le Page, G. Donnay, *Acta Crystallogr. Sect. B* **1976**, *B32*, 2456–2459.
- [24] A. M. Ferrari, E. Garrone, G. Spoto, P. Ugliero, A. Zecchina, *Surf. Sci.* **1995**, *323*, 151–162.
- [25] Extrapolated by hyperbolic fit: $y = a + b/x$
- [26] N. H. de Leeuw, Z. Du, J. Li, S. Yip, T. Zhu, *Nano Lett.* **2003**, *3*, 1347–1352.
- [27] A modified 6–21G* basis set was applied for carbon, see: M. Catti, A. Pavese, R. Dovesi, V. R. Saunders, *Phys. Rev. B* **1993**, *47*, 9189–9198.
- [28] H. Kietzmann, R. Rochow, G. Ganteför, W. Eberhardt, K. Vietze, G. Seifert, P. W. Fowler, *Phys. Rev. Lett.* **1998**, *81*, 5378–5381.
- [29] a) R. O. Jones, *J. Chem. Phys.* **1999**, *110*, 5189–5200; b) Z. Chen, H. Jiao, M. Bühl, A. Hirsch, W. Thiel, *Theor. Chem. Acc.* **2001**, *106*, 352–363; c) B. Paulus, *Phys. Chem. Chem. Phys.* **2003**, *5*, 3364–3367.
- [30] B. I. Dunlap, D. W. Brenner, J. W. Mintmire, R. C. Mowrey, C. T. White, *J. Phys. Chem.* **1991**, *95*, 8737–8741.
- [31] J. Aihara, *Phys. Chem. Chem. Phys.* **2000**, *2*, 3121–3125.
- [32] R. G. Pearson, *J. Am. Chem. Soc.* **1988**, *110*, 2092–2097.
- [33] Z. A. Weinberg, G. W. Rubloff, E. Bassous, *Phys. Rev. B* **1979**, *19*, 3107–3117.

Received: June 21, 2005
Published online: October 26, 2005